Democratizing access to microfluidics: Rapid prototyping of capillary microfluidics with a low-cost masked stereolithography 3D printer

Authors:

Kelsey M. Leong[1]

Mindy L. Quach*[1]

Carrie H. Lin*[1]

Cosette A. Craig*[1]

Aileen Y. Sun[2]

Felix Guo[1]

Timothy R. Robinson[1]

Ayokunle O. Olanrewaju [1, 2]

*contributed equally

1. Department of Mechanical Engineering, University of Washington, Seattle WA
2. Department of Bioengineering, University of Washington, Seattle WA

Abstract

Capillary microfluidic devices provide minimally-instrumented and user-friendly liquid handling for a range of biochemical applications. 3D printing is an attractive method for microfabricating capillary microfluidics because it requires little training, is cost-effective compared to conventional cleanroom fabrication, and can drastically decrease prototyping time. High-resolution (≤ 100 μm) microfluidics are typically 3D printed using digital light projection

(DLP) stereolithography (SLA); however, the high capital cost (>$10,000) of high-resolution DLP-SLA printers limits their accessibility and widespread use. Recent advances in liquid crystal display (LCD) technology have provided inexpensive (<$500) masked stereolithography (mSLA) 3D printers with sufficient optical resolution for microfluidics. Despite their potential, there have only been a few demonstrations of microfluidic fabrication with mSLA printers, limited characterization of the effects of printing parameters like UV power and exposure time on print quality, and no direct comparisons with DLP-SLA printing. We compared a 40-μm pixel resolution DLP-SLA printer (~$18,000) with a 34.4-μm pixel resolution (~$380) mSLA printer. When printing with the same resin and optimized parameters for each printer, the DLP-SLA printer produced features with an average 4.8% difference between designed and measured XY dimensions and a coefficient of variation [CV] = 2.17 ± 2.53% (N=3). The 34.4 μm mSLA printer produced features that were 15.3 ± 11.4% larger than designed dimensions, although they were very precise [CV = 1.80 ± 1.11%, N =3]. Using a low-cost, water-wash resin optimized for the mSLA printer, microchannels printed with the mSLA differed from designed dimensions by only 4.20 ± 4.83%. To demonstrate that we could optimize print conditions for multiple mSLA printers, we printed microchannels with a 22 μm mSLA printer (~$450) and obtained features that were on average 2.43 ± 5.88% different from designed dimensions. We 3D-printed capillary microfluidic circuits – composed of stop valves, trigger valves, retention burst valves, retention valves, and domino valves – for automating sequential delivery of five liquids. Taken together, our results show that mSLA printers are an inexpensive alternative for fabricating capillary microfluidics with minimal differences in fidelity and accuracy of features compared with a 20X more expensive DLP-SLA printer.

Introduction

Capillary microfluidics use surface tension effects defined by microchannel geometry and surface chemistry to achieve self-powered and self-regulated flow with applications ranging from diagnostics[1–3] to electronics.[4] Despite their potential to democratize access to fluid handling in a variety of settings regardless of instrument availability or financial capability, the high cost and centralization of microfabrication technology have limited the widespread deployment of capillary microfluidics. The history of capillary microfluidics fabrication has been thoroughly reviewed elsewhere,[5] highlighting the progression from expensive and time-consuming methods, such as cleanroom fabrication, towards more economical and rapid prototyping methods like 3D printing. The swift and frugal prototyping offered by 3D printing, as well as the ease of realizing features with complex 3-dimensional structures, accelerates discovery. For instance, *capillaric* circuits – capillary microfluidics designed using electrical analogies and consisting of multiple fluidic elements – have recently been developed to enable pre-programmed and scalable delivery of liquids in a “walk-away” format.[6] After the user loads reagents into reservoirs, capillaric fluidic elements including trigger valves, retention burst valves, and domino valves control the sequence and timing of liquid delivery without additional user intervention. 3D-printed capillaric circuits have been designed for user-friendly and instrument-free sequential delivery of 300 liquids, and applications including automation of COVID-19 antibody screening and blood coagulation cascades.

Prior work[7] compared different 3D printing technologies, with the goal of achieving rapid and cost-effective prototyping microfluidic devices. Those findings indicated that stereolithography (SLA) based 3D printing yielded high-fidelity and high-resolution microchannels. Digital light processing (DLP) SLA, using high-resolution projectors, has become the gold standard[8–10] for 3D printing microfluidics and features with cross sections as small as 18 μm X 20 μm have been

reported.[11] DLP-SLA 3D printers tailored specifically for microfluidics applications have even been developed and commercialized.[12] Despite the potential to democratize access to fluid handling in various settings regardless of instrument availability or financial capability, initial acquisition costs of high-resolution DLP-SLA printers are prohibitive (typically ≥ $10,000), especially in low- and middle-income settings. This precludes access to those who might most need the minimally-instrumented and semi-automated fluid handling offered by capillary microfluidics, since many well-resourced laboratories can readily automate their fluid handling processes using expensive liquid handling robots.

Recent advances in 3D printing technology and liquid crystal displays (LCDs) have provided access to masked stereolithography (mSLA) printers with high resolution and low cost. mSLA printing uses LCD screens instead of projectors to modulate illumination of photosensitive resin (**Figure 1a**).[13,14] Over the past decade, advancements in LCD technology, spearheaded by the inclination to improve the resolution of smartphone, tablet, and computer displays, have equalized efficiency and print quality between mSLA printers and DLP-SLA printers.[15] Whereas mSLA printing has traditionally been relegated to hobbyists requiring low-cost, smaller footprint, but not necessarily high-resolution printers, these recent improvements in LCD technology have leveled the playing field in print quality for mSLA and DLP-SLA printers. Although there are reports of fabrication of molds for microfluidic devices,[16–18] and direct 3D printing of microstructures,[19–23] there is limited characterization of the effects of printing parameters like UV power and exposure time on print quality with mSLA printers, and no direct comparisons with DLP-SLA printing. Given that these low-cost mSLA printers are not specifically designed for microfluidics, they also do not have the dedicated documentation and customer service teams to troubleshoot creation of small microfluidic features. As such, additional optimization and process development is required to print high-resolution and high-fidelity microfluidics with mSLA printers.

In this manuscript, we describe optimized parameters for the fabrication of capillary microfluidics using two commercially available and inexpensive (<$500) mSLA printers and compare their capabilities with a DLP-SLA printer designed for microfluidic fabrication. We optimized print parameters – exposure time, layer height, off time, and UV power – on the mSLA printers until we found settings that produced high-resolution and high-fidelity features. We compared the measured and designed XY and Z dimensions of a standardized calibration microchip for the mSLA and DLP-SLA printers. We demonstrated the functionality of mSLA printing by microfabricating a capillaric circuit with domino valves for sequential, instrument-free, and hands-free delivery of multiple liquids.

Materials and Methods

Equipment & Software

We compared the performance of a commercially available DLP-SLA printer (CADWorks Profluidics 285D) with two mSLA printers, the Anycubic Mono X 6K and the Phrozen Sonic Mini 8K, to confirm that we could find optimal parameters for printing microfluidic devices on more than one mSLA printer. Microchannels and microfluidic circuits were designed using Solidworks (Waltham, Massachusetts, USA) and exported as Standard Tessellation Language (STL) files prior to 3D printing. The following printer and STL slicer combinations were used: Profluidics 285D printer and the CADworks Utility 6.44 slicer (CADworks3D, Toronto, Ontario, Canada), Anycubic Photon Mono X 6K and the Anycubic V2.1.29 slicer (Anycubic, Shenzhen, Guangdong, China), and the Phrozen Sonic Mini 8K Resin 3D printer (Phrozen, Hsinchu, T'ai-wan, Taiwan) and Chitubox Basic 1.9.5 slicer (Chitubox, Shenzhen, Guangdong, China). Microchips were plasma treated with the Plasma Etch PE-25 (Carson City, Nevada, USA) at 56% power for 3 minutes to achieve a hydrophilic surface for capillary-driven flow. Image

capture, XY measurements **(Supplementary Figure 1)**, and surface profiling were performed with the Keyence VH-S30B digital microscope (Itasca, Illinois, USA). Image capture and height measurements were performed using the FEI XL30 Sirion scanning electron microscope (SEM) (Hillsboro, Oregon, USA). Videos of liquid delivery in the microfluidic chip were taken using an iPhone XS (Apple, Cupertino, CA, USA).

Materials

The goal of this study was to characterize printer hardware rather than different resin formulations. The following commercially available resins were used in the printer optimization experiments: Clear Microfluidics Resin V7.0a (CADworks3D, Toronto, ON, Canada) and Water-Wash Resin+ (AnyCubic, Shenzhen, Guangdong, China). Isopropanol was sourced from Sigma-Aldrich (Burlington, Massachusetts, USA), and colored food dyes (Watkins, Winona, Minnesota, USA) were employed for flow characterization in 3D printed capillaric circuits.

Evaluation of dimensional accuracy using pixel calibration chips

Pixel calibration chips of microchannels with varying widths and heights were fabricated to test the 3D printer resolution limitations **(Figure 1b)**. The calibration chips' outer dimensions were 26.8 mm in length x 18.9 mm in width x 2.5mm in height. The pixel chip designed made for the Anycubic Mono X 6K printer was designed to test the XY resolution of 34.4 μm,[24] while the pixel chip designed for the Phrozen Sonic Mini 8k printer was designed to test the XY resolution of 22 μm.[25] The channels on the pixel calibration chip were aligned with each mSLA printer's pixel grid **(Figure 1a)** to avoid errors associated with features that fell between gridlines and could not be sliced or printed properly with the mSLA printers.

Pixel calibration chips had channels with widths ranging from 1-10 pixels increasing in whole pixel increment steps at a uniform z-height of 160 μm. The channels for each pixel size were

printed in triplicate. Although printing channels in the 1-3 pixel range is not within the capabilities of many commercial printers,[11] collecting this information can tell us more about the limitations of each printer. To test the z-height resolution, we fixed the XY channel size to 5 pixels and increased channel depth from 20 µm to 180 µm in 40 µm increments. Channels at each z-height were printed in triplicate.

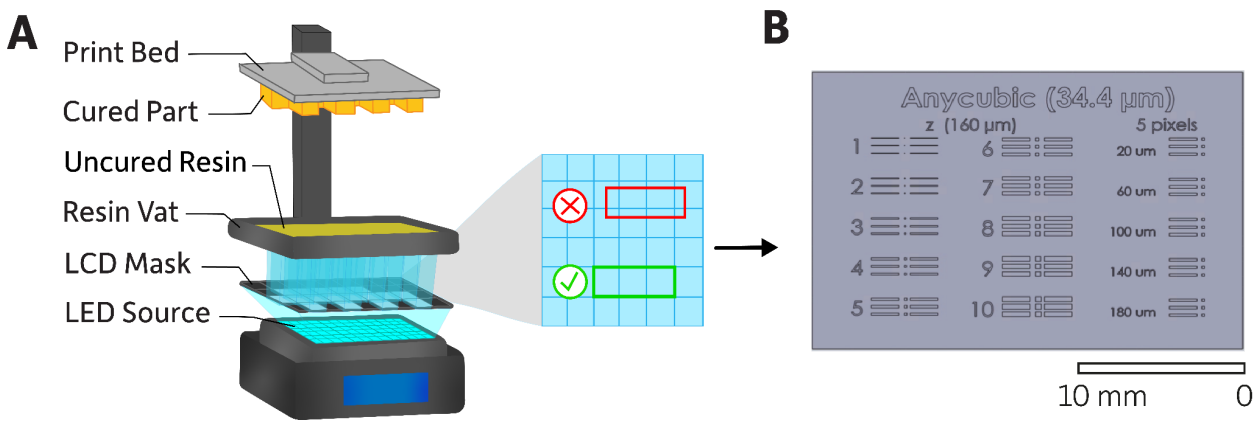

Figure 1: mSLA printer schematic with pixel grid alignment and pixel calibration chip with varying XY and z-heights.

(a) Schematic showing mSLA printer components. The LCD mask has a discrete pixel grid. To the right, the pixel grid is depicted with a misaligned feature shown with a red rectangle and a correctly aligned feature shown with a green rectangle. Misalignment to the grid can decrease print accuracy. **(b)** CAD design of the pixel calibration chip designed for the 34.4 µm mSLA printer. The first two columns are channels with fixed height (160 µm) and XY dimensions ranging from 1 pixel (34.4 µm) to 10 pixels (344 µm) in 1-pixel increments. The third column (far right) has features with fixed width (5 pixels) and heights varying from 20 µm to 180 µm in 40 µm increments.

Pixel calibration chip designs were exported as STL files, converted into G-code with their respective slicers, and 3D printed. The chips printed with the CADworks resin were washed in an isopropanol (IPA) bath to remove excess resin and dried using a compressed nitrogen gun (Cleanroom World, Centennial, Colorado, USA). In contrast, chips printed with the Anycubic Water-Wash Resin+ were washed in a deionized water bath to remove excess resin and dried

using a compressed nitrogen gun. The washing and drying steps were repeated, as needed, for both resins to ensure that any remaining uncured resin was removed from the part. After drying, the microchips were placed in a Formcure (Formlabs, Somerville, Massachusetts, USA) to post-cure for 30s on each side of the chip, for a total of 1 minute.

Capillaric circuits for pre-programmed instrument-free liquid delivery

Capillaric circuits were fabricated to test the performance of the 3D printed parts and showcase a variety of capillaric fluidic elements that enable hands-free and minimally-instrumented liquid delivery. Once printed, the chips were washed, dried, and post-cured in the same manner described above. After post-curing, the chips were plasma-treated and sealed with hydrophobic tape (ARseal™ 90697, Adhesives Research, Glen Rock, Pennsylvania, USA). 1 mL of deionized water was mixed with 3 drops of food coloring to test flow rate conditions. Non-woven cleanroom paper (AAWipes, Ann Arbor, Michigan, USA) was used as the capillary pump and fastened to the capillaric circuit using a rubber band.

Results and Discussion

The specifications for the DLP and mSLA printers used in this study are summarized in **Table 1**. Among the three printers, the Phrozen printer has the lowest documented XY pixel size at 22 µm, followed by the CADworks dynamic pixel size of 28.5 µm, the Anycubic pixel size of 34.4 µm, and the CADworks native pixel size of 40 µm. The mSLA printers have a lower weight, smaller profile, and are much (≥40X) less expensive than the DLP-SLA printer. The mSLA printers operate at 405 nm, while the DLP-SLA printer operates at 385 nm.

Table 1: Comparison of specifications for the DLP-SLA and mSLA printers tested

	3D-Printer		
	CADworks Profluidics 285D	Anycubic Mono X 6K	Phrozen Sonic Mini 8K

Printing method	Digital Light Processing (DLP)	Masked Stereolithography (mSLA)	mSLA
Pixel Resolution	2,750 x 1,550 pixels	5,760 x 3,600 pixels	7,536 x 3,240 pixels
Pixel size	40 µm (native) 28.5 µm (dynamic)	34.4 µm	22 µm
Build area XYZ (mm)	110 mm x 62 mm x 120 mm	245 mm x 197 mm x 122 mm	165 mm x 72 mm x 180 mm
Operating wavelength	385 nm	405 nm	405 nm
Light intensity	5 - 6 mW/cm^2	5 - 6.5 mW/cm^2	2.8 mW/cm^2
Instrument footprint XYZ	500 mm x 570 mm x 590 mm	475 mm x 290 mm x 270 mm	290 mm x 290 mm x 430 mm
Instrument Weight	56 kg	11 kg	13 kg
Cost (USD)*	$17,995	$382	$449.99

*Documented price as of 9/8/23

Evaluation of dimensional accuracy using pixel calibration chips

Initial optimization of print parameters on mSLA printers

We systematically varied printing parameters including UV power, exposure time, layer height, retraction speed, off-time, and anti-aliasing to determine the best conditions for printing sub-millimeter, negative features with a minimum overall print time. We designed a standardized pixel calibration chip for each mSLA printer (**Figure 1b**). The manufacturer's recommended settings for each mSLA printer are well suited for printing larger (> 1 mm) features and have not been validated for printing microfluidic features. We found that channel walls were more corrugated as UV power increased on the 34.4 µm mSLA printer **(Figure 2)**. We chose a UV power of 45% that provided straight side walls without excess uncured resin on the microchannel surface.

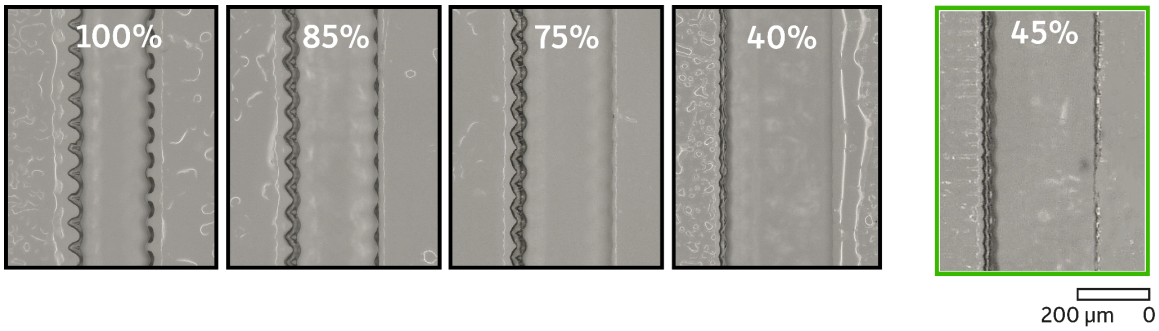

Figure 2: 3D-printed channels at different UV power settings on an mSLA printer. We screened UV power ranging from 40% up to 100%. We chose a UV power of 45% because the channel sidewalls demonstrated the least amount of corrugation while also having a minimum amount of uncured resin on the channel surface.

We found that an exposure time of 1.8 seconds produced higher fidelity negative features than the manufacturer's recommended setting of 2 seconds. Furthermore, increasing the off-time, the time between when the build platform is completely lowered into the resin vat and when the UV light is turned on, from the recommended 0.5 seconds to 1 second improved the quality of our prints. Our optimized printing parameters for both mSLA printers are summarized in **Supplementary Table 1**. At equivalent layer heights of 20 µm, both the DLP-SLA and 34.4 µm mSLA printer produced the same pixel calibration chip in < 34 minutes.

3D printing with identical resin on DLP-SLA and 34-µm pixel mSLA printer

We printed the same pixel calibration chip with CADworks resin on both the 40-µm pixel DLP-SLA printer and 34.4 µm mSLA printer. SEM photos (**Figure 3**) provide qualitative comparisons between microchannels produced with the printers. For XY feature comparisons, we fixed microchannel depth at 160 µm (13 layers) and systematically varied XY feature widths from 1 to 10 pixels. For both printers, the 1 pixel channels were poorly defined. The 2 and 3 pixel features were better defined, although they lost dimensional integrity near channel edges and resembled comet or brush stroke shapes. Besides slight rounding on channel endpoint

corners, features above 3 pixels did not have any noticeable defects. This is similar to prior work with DLP-SLA where minimum microchannel widths were ~4X the printer's minimum pixel size.[11]

Microchannel dimensions from the DLP-SLA printer **(Figure 3b)** strongly correlated with designed dimensions above 3 pixels (103.2 μm). The difference between designed and measured widths was ≤ 4.8%, with an average error of 2.74 ± 1.81% for channels ranging from 3 pixels (103.2 μm) to 10 pixels (344 μm). Channels printed with the DLP-SLA printer were very precise with average coefficient of variation [CV] of 2.17 ± 2.53% across three replicate channels on the same pixel calibration chip. While the pixel calibration chip was designed for the Anycubic mSLA's 34.4 μm pixel size, these results demonstrate that the DLP-SLA printer was still able to produce accurate feature sizes due to its dynamic printing capabilities.

Microchannels printed with the 34.4-μm pixel mSLA printer were larger than those obtained with the DLP-SLA printer (and the designed dimensions). The average difference between measured and designed dimensions for the 34.4-μm pixel mSLA printer was 20.5 ± 3.42% for features ≥ 3 pixels (103.2 μm). Nevertheless, replicated microchannels (N=3) on the mSLA printer were very precise for each pixel size with an average CV of 1.8 ± 1.11%. XY measurements from the mSLA printer also showed consistent linearity for features ≥ 3 pixels.

We compared channel depths with features that had fixed microchannel widths of 5 pixels to avoid inaccuracies related to unresolved microchannel widths with smaller features. There was consistent linearity in microchannel depths from the DLP-SLA printer **(Figure 3c)** for channels at depths of 3 layers (60 μm), 5 layers (100 μm), 7 layers (140 μm), and 9 layers (180 μm). However, 1-layer (20 μm) channels had significantly larger deviation from the designed dimensions. Features ≥ 3 layers (60 μm) had an average difference of 4.36 ± 3.95% between

measured and designed dimensions. There was minimal variation between depths of triplicate microchannels printed on the same pixel calibration chip with an average CV = 3.85 ± 2.00%.

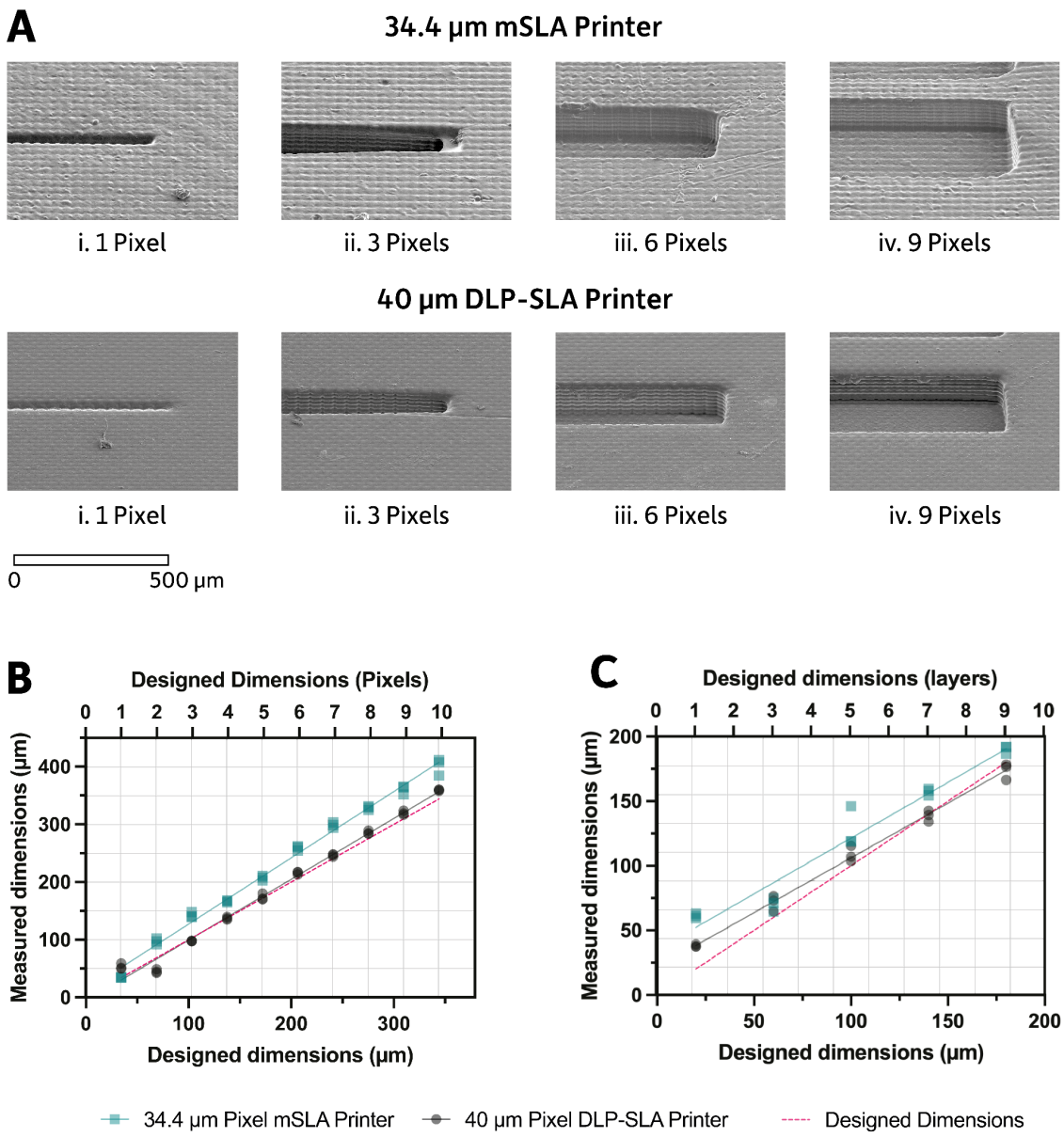

Figure 3: Comparison between microchannels printed with the same resin on 34.4-µm pixel mSLA and 40-µm pixel DLP-SLA printers.

(a) SEM images show that deep microchannels (160 µm height; 13 layers) printed with the 34.4-µm pixel mSLA and the 40-µm pixel DLP-SLA printers had high fidelity above 3 pixels in width. **(b)** Microchannels printed with the DLP-SLA had excellent agreement between designed and measured widths, while channels from the 34.4-µm mSLA printer were larger but maintained a good linear trend as pixel size increased. **(c)** Microchannel depths from both the

DLP-SLA and mSLA overestimated designed depths, although both maintained linear trends as layer height increased.

The 34.4-μm pixel mSLA printer had a similar depth profile to the DLP-SLA printer **(Figure 3c)**. There was good linearity and lower variation between designed and measured dimensions above 3 layers (60 μm) depth. The deviation between measured and designed depths was on average 15.3 ± 11.4%, greater than the ~4% observed with the DLP-SLA printer. There was minimal variation between depths of triplicate microchannels printed on the same pixel calibration chip with an average CV of 4.18 ± 3.80%. Taken together, our width and depth measurements indicate that the 34.4-μm pixel mSLA printer can fabricate microchannels that are suitable for many microfluidic applications including capillaric fluid handling.

3D printing with 22-μm pixel mSLA printer

To demonstrate reproducible microfluidic fabrication across two different printers, we designed and printed a pixel calibration chip on a 22-μm pixel mSLA printer (Phrozen Sonic Mini 8K) and evaluated. We used the same commercial resin, Clear Microfluidics Resin V7.0a (CADworks3D, Toronto, Ontario), as in our earlier work with the DLP-SLA and 34.4-μm pixel mSLA printers. Unlike the 34.4-μm pixel resolution mSLA printer that we tested, the 22-μm pixel mSLA printer did not allow us to vary UV power; however, we modified exposure time to obtain high fidelity and accuracy of printed features (**Supplementary Table 1**).

Microchannels printed with the 22-μm mSLA printer **(Figure 4)** looked very similar to those obtained with the DLP-SLA and the 34.4 μm mSLA printers. Microchannel widths seemed to plateau below 3 pixels (66 mm) wide **(Figure 4B).** Subsequently, increases in designed widths resulted in commensurate increases in measured dimensions following an overall linear trend. For microchannels ≥ 3 pixels (66 μm), the average difference between designed and measured

widths was 2.43 ± 5.88%. Microchannel depths followed a similar pattern with an average difference of ~2% between measured and designed dimensions **(Figure 4B).** These results suggest that we can optimize two different mSLA printers for printing microchannels with sizes and aspect ratios relevant to capillary microfluidics applications. Our approach may be broadly generalizable to other mSLA printers with similar pixel resolution and price points.

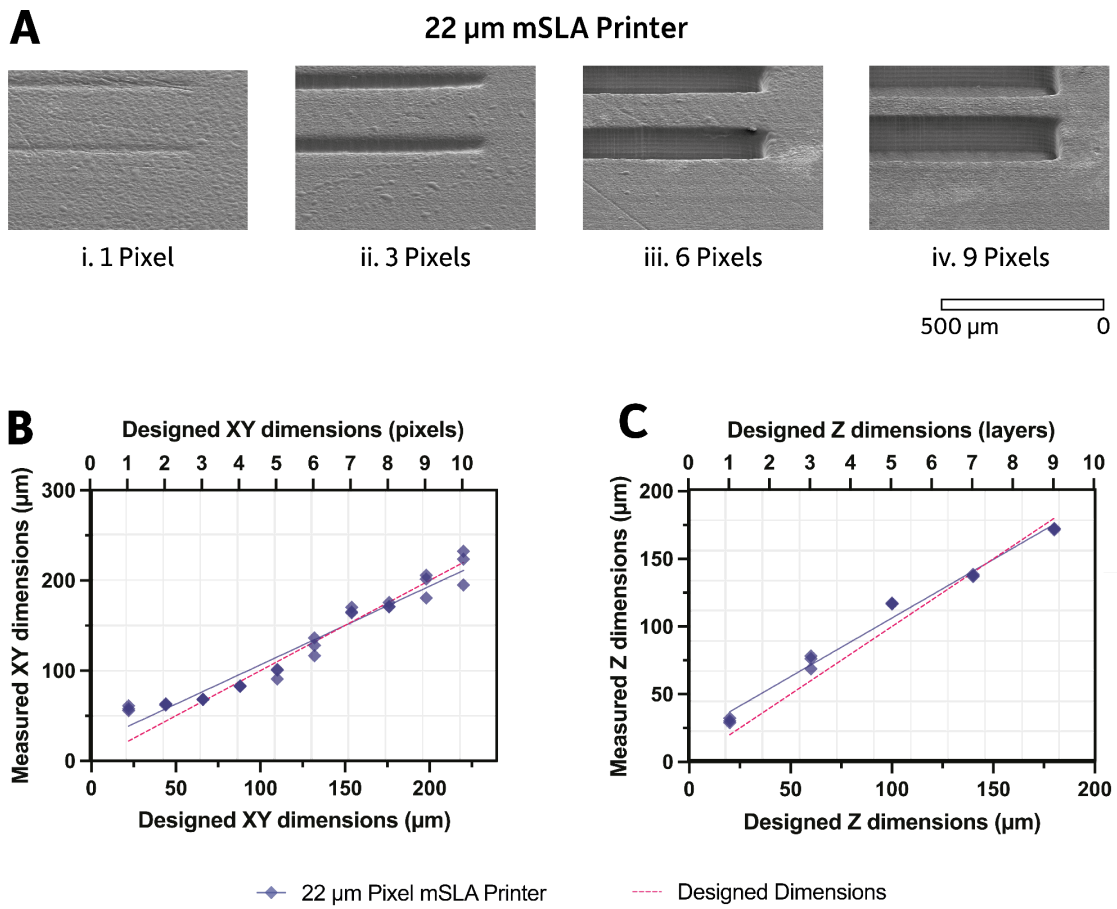

Figure 4: 3D-printed microchannels with 22-µm pixel mSLA printer.
(a) SEM images show that deep microchannels (160 µm height; 13 layers) had high fidelity above 3 pixels in width. **(b)** Microchannels printed with the DLP-SLA had excellent agreement between designed and measured widths above 3 pixels. **(c)** Measured depths of 3D printed microchannels followed a linear trend with increasing layer height and only slightly overestimated designed dimensions.

3D printing with low-cost, water-wash resin on mSLA printer

Our initial optimization (**Figures 3 and 4**) used commercially available Clear Microfluidics Resin V7.0a (CADworks3D, Toronto, Ontario) that cost $510/kg and was cleaned using IPA. To decrease operating costs and reduce chemical/hazardous waste disposal concerns, we tested a low-cost ($34/kg) water-wash resin on the 34.4-μm pixel mSLA printer.

Compared to microchannels printed with the IPA wash resin on the same printer, (**Figures 3a**), channels printed with the low-cost water-wash resin had less rounded edges and appeared a little smaller (**Figures 5a**). Although we noticed some edge defects on the channels, similar to prints with IPA-wash resin, the low-cost water-wash resin provided microchannels with more accurate channel widths and depths. Microchannels printed with the water-wash resin had excellent agreement between measured and designed widths, with an average difference of 4.20 ± 4.83% across all channel widths tested (**Figures 5b**). Although the 1-layer (20 μm) deep channel printed much larger than the designed dimension, the average difference between designed and measured depths for features ≥ 3 layers (60 μm) was 3.72 ± 6.55% (**Figures 5b**). We hypothesize that these improvements in print quality with the low-cost water-wash resin compared with the IPA-wash resin are likely because the water-wash resin (Water Wash+, AnyCubic, Shenzhen, Guangdong, China) was designed for mSLA printers that operate at 405 nm, meanwhile the IPA-wash resin (Clear Microfluidics Resin V7.0a, CADworks3D, Toronto, ON, Canada) was tailored for printers at 385 nm but could also be used at 405 nm. These results highlight the importance of optimizing print settings for each resin type.

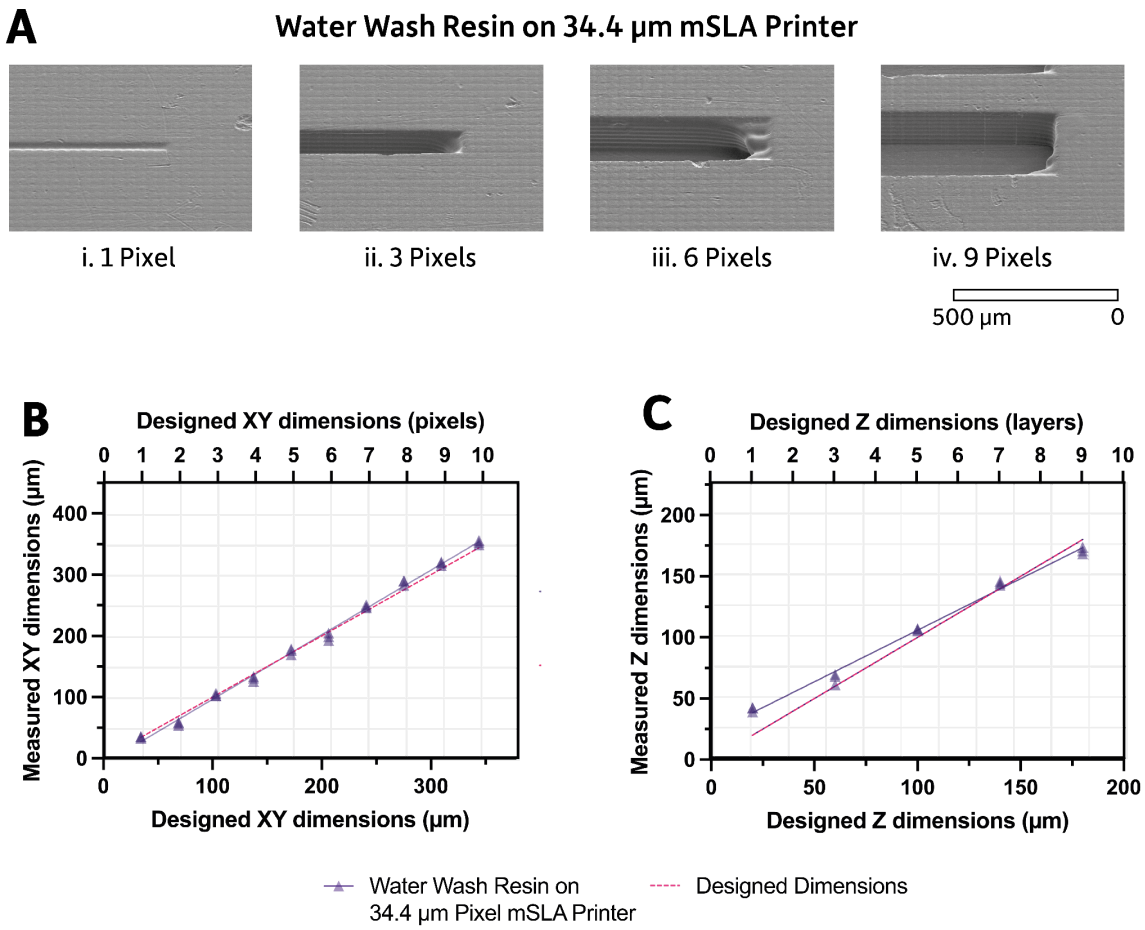

Figure 5: 3D-printed microchannels with low-cost, water-wash resin on mSLA printer. **(a)** SEM images show well defined microchannels with some edge defects. **(b)** Microchannels printed with the water-wash resin had excellent agreement between designed and measured widths, with an average difference of 4.20 ± 4.83% across all pixel sizes. **(c)** Measured depths followed a linear trend with increasing layer height with an average difference of 3.72 ± 6.55% between designed and measured dimensions above 3 layers (60 µm).

Limitations of dimensional comparisons between DLP-SLA and mSLA

Although the results in **Figures 3, 4, and 5** show excellent agreement between designed and measured microchannel widths and depths with mSLA printers, our work has a few limitations. First, we did not test an exhaustive range of width and depth combinations for the microchannels presented here. Instead we tested dimensions that are reasonable and typical for capillary-driven flow operations. In addition, we only printed open microchannels that were

sealed with adhesive tape and did not test fully embedded microchannel. Again, this was in keeping with our intended application of demonstrating capillary-driven flow in microchannels where sealing with a hydrophobic cover helps to improve the robustness of capillary trigger valves.

Pre-programmed, Instrument-free Liquid Delivery with Capillaric Circuit

We designed capillaric circuits composed of multiple fluidic elements (**Figure 6A**) to demonstrate the functionality of microchannels fabricated with the mSLA printers. CAD designs were aligned to the pixel grid and printed using water wash resin on the 34.4 µm mSLA printer. The smallest features in the capillaric circuit were the trigger valve, retention valve, and flow resistor, which had XY features ranging from 5 - 6 pixels and z-heights of 200 µm. There was slight narrowing of the flow resistor as shown (**Figure 6B**), but otherwise there were no obvious defects. The printer produced each component with accurate geometries with consistency across multiple chips.

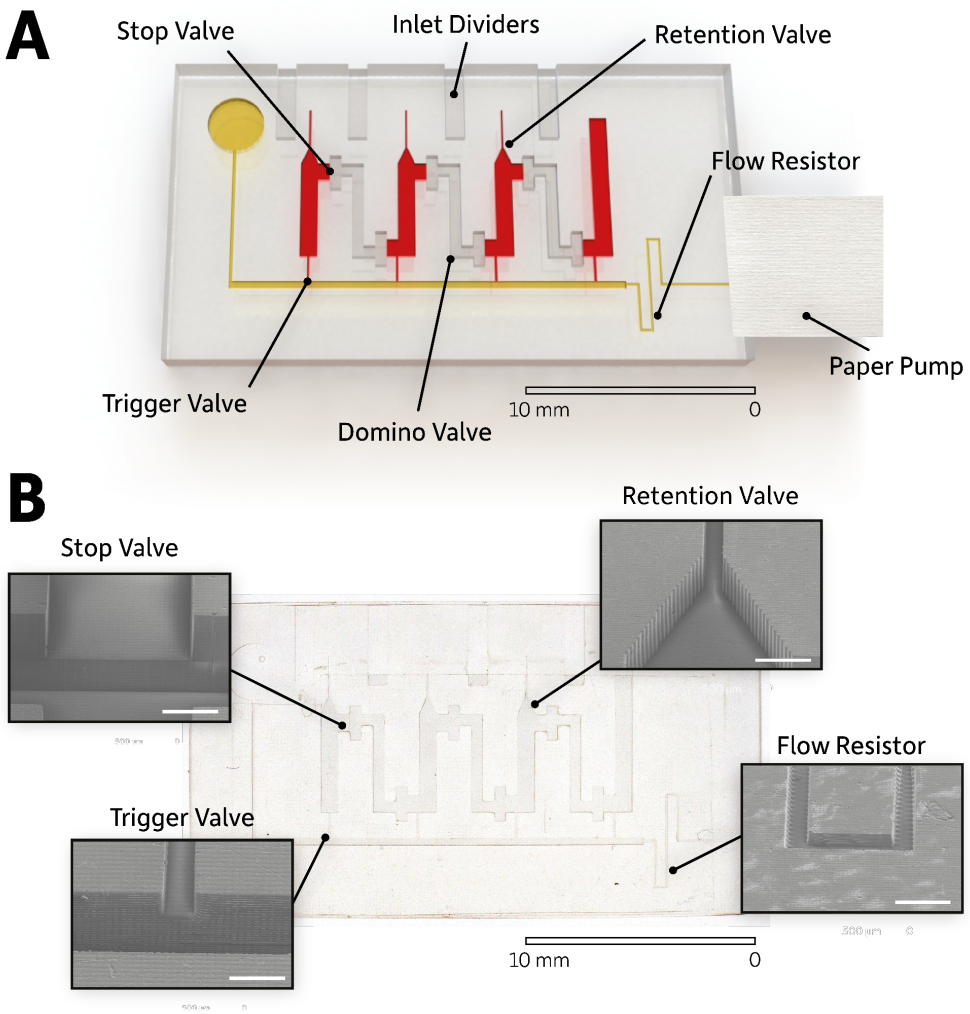

Figure 6: Capillaric circuit printed with water wash resin using 34.4 µm mSLA printer. **(a)** CAD schematic depicting the design of the capillary domino valve circuit. Four features noted are the i. Stop valve, ii. Retention valve, iii. Trigger valve, and iv. Resistor. The paper pump is attached to the end of the resistor. The reservoirs are filled in with red and the main channel is filled in with yellow. **(b)** The 3D printed circuit is shown in the center and blown-up SEM images of the dynamic components are shown in the periphery; i. Stop valve, ii. Retention valve, iii. Trigger valve, and iv. Resistor. Scale bars on SEM images are 500 µm.

Three capillaric circuits were printed, plasma treated, and tested to demonstrate replicable automated, sequential liquid delivery performed on mSLA printed microchips. Operation of capillaric circuits follows our previous work describing the principle of operation of capillary

domino valves.[6] Screenshots from a video of liquid handling in the capillaric circuit (**Supplementary Video 1**) are shown in **Figure 7A**. First, the user loads liquids in the reservoirs where trigger valves hold liquid in place (**Figure 7A.1.**) until pre-programmed sequential liquid delivery is initiated by loading the control channel that connects the reservoirs to the capillary pump (**Figure 7A.2.**). Unlike reservoirs 2, 3, and 4 that have retention valves preventing their immediate drainage, reservoir 1 immediately drains when connected to the capillary pump (**Figure 7A.3.**). When reservoir 1 is empty, the domino valve connecting reservoirs 1 and 2 enables drainage of reservoir 2 (**Figure 7A.4.**). This triggers a domino effect where each reservoir drains once the preceding reservoir is completely empty (**Figure 7A.5 & 6.**).

To demonstrate reproducibility of fluid delivery with capillaric circuits fabricated with mSLA printers, we compared the flow rates from each reservoir across 3 different microchips (**Figure 7B**). Reservoirs 1, 2, 3, and 4 had consistent average flow rates of 0.12 ± 0.03 μL/s, 0.11 ± 0.03 μL/s, 0.10 ± 0.01 μL/s, and 0.10 ± 0.01 μL/s, respectively, across all three 3D-printed capillaric circuits. These results show that we can fabricate a functional capillaric circuit for hands-free and instrument-free liquid delivery using an inexpensive mSLA printer.

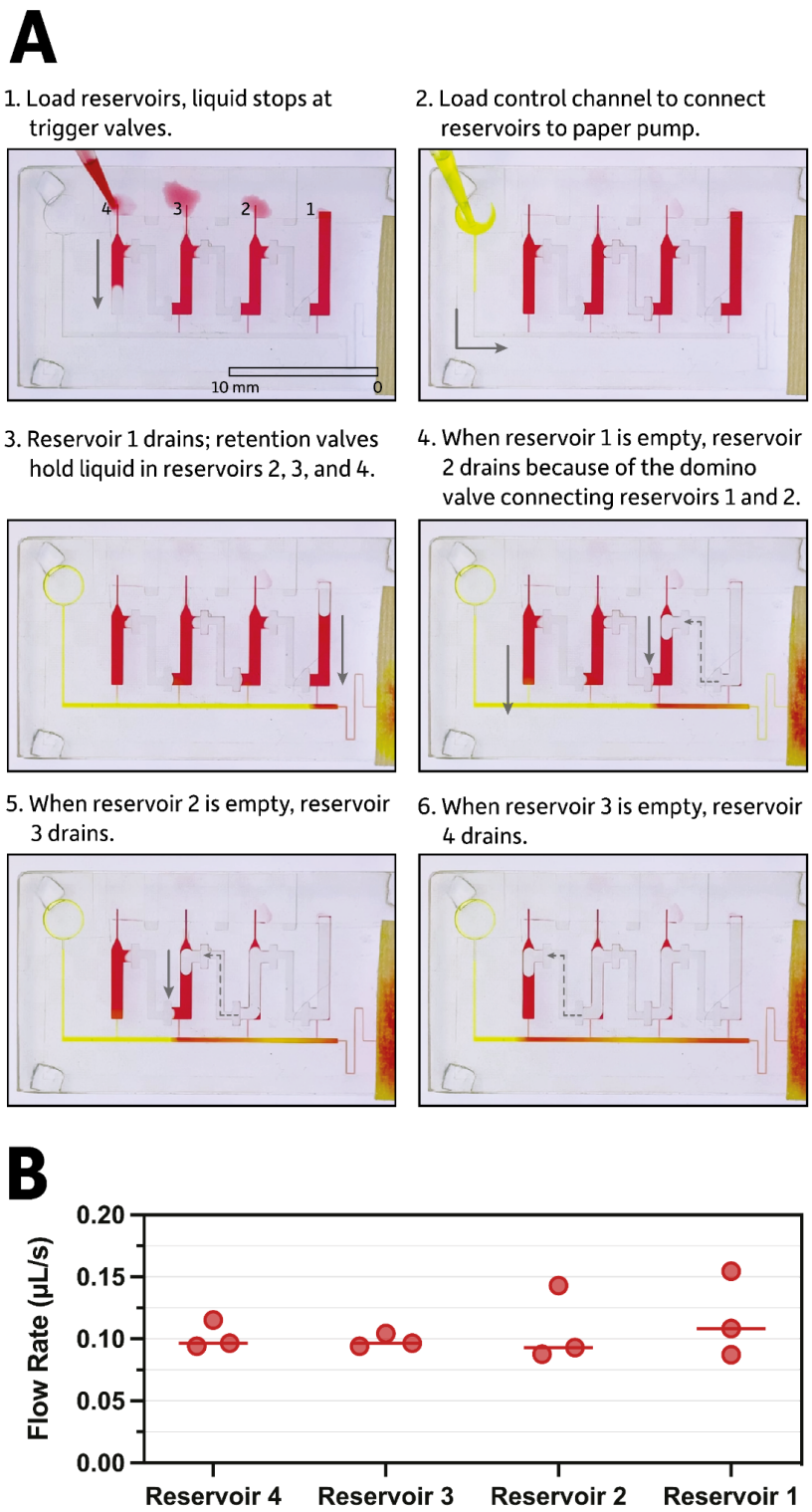

Figure 7: Pre-programmed, instrument-free, sequential liquid delivery with capillaric circuit 3D-printed with low-cost, water-wash resin on 34.4 µm mSLA printer.

(a) Screenshots from supplementary video 1 showing pre-programmed, instrument-free liquid delivery in capillaric circuit. The screenshots progress from loading of the liquids into the

reservoirs and control channel (1,2), through the drainage of each sequential reservoir (3 – 6). **(b)** Flow rates were consistent across all reservoirs and depict minimal variability across three 3D-printed microchips.

Conclusion

In this paper, we demonstrate that a suitable trade-off can be found between 3D-printer cost and microchannel fidelity and accuracy for capillary microfluidics applications. We compared a DLP-SLA printer (~$18,000) and two mSLA printers (<$500) and obtained excellent agreement between designed and measured dimensions for all printers. We optimized print settings including UV power and exposure time to increase the fidelity and accuracy of features produced by the mSLA printers. We also showed that multiple commercially available 3D printing resins, including a low-cost ($30/liter) water-wash resin could be used to fabricate high-fidelity microchannels. This flexibility may allow researchers to test resins with different material properties, such as elasticity, hydrophilicity, optical clarity, or biocompatibility to broaden their functionality for biomedical applications. This work expands on prior work showing microfluidic fabrication with mSLA printers by providing a direct comparison with a high-resolution DLP-SLA printer, and demonstrating the realization of functional capillaric circuits for autonomous liquid delivery. This validation of frugal 3D-printing for capillary microfluidics could increase access to semi-automated, minimally-instrumented, and high-throughput fluid handling to researchers with limited budgets and citizen scientists.

Author Contributions

K.L. was involved in the conceptualization, methodology, investigation, validation, formal analysis, data curation, project administration, and completed the initial draft. M.Q. and F.G. assisted with conceptualization, investigation, and data curation. C.C. and C.L. helped with visualization, paper editing, and software, and C.L. aided with investigation. A.S. participated in

investigation, formal analysis, and data curation. T.R. contributed to paper edits and supervision. A.O. provided supervision and aided with methodology, funding acquisition, conceptualization, and paper editing.

Acknowledgments

We are grateful to Ashleigh Theberge, Jodie Tokihiro, Yuting Zeng, Dan Ratner, Lucas Meza, for helpful comments and support.

Funding Information

We are grateful for funding from the Atlanta Center for Microsystems Engineered Point-of-Care Technologies and the National Science Foundation (Award #2223537). Part of this work was conducted at the Washington Nanofabrication Facility / Molecular Analysis Facility, a National Nanotechnology Coordinated Infrastructure (NNCI) site at the University of Washington with partial support from the National Science Foundation via awards NNCI-1542101 and NNCI-2025489. We acknowledge equipment support from the M.J. Murdock Diagnostics Foundry for Translational Research and the Molecular Analysis Facility at the University of Washington.

Data Availability

Link to CAD files, raw data (images), and Excel sheets for image analysis:
https://doi.org/10.5281/zenodo.8347134

References

(1) Hassan, S.; Tariq, A.; Noreen, Z.; Donia, A.; Zaidi, S. Z. J.; Bokhari, H.; Zhang, X. Capillary-Driven Flow Microfluidics Combined with Smartphone Detection: An Emerging Tool for Point-of-Care Diagnostics. *Diagnostics* **2020**, *10* (8), 509. https://doi.org/10.3390/diagnostics10080509.

(2) Zimmermann, M.; Hunziker, P.; Delamarche, E. Autonomous Capillary System for One-Step Immunoassays. *Biomed. Microdevices* **2009**, *11* (1), 1–8. https://doi.org/10.1007/s10544-008-9187-2.

(3) Novo, P.; Chu, V.; Conde, J. P. Integrated Optical Detection of Autonomous Capillary Microfluidic Immunoassays:A Hand-Held Point-of-Care Prototype. *Biosens. Bioelectron.* **2014**, *57*, 284–291. https://doi.org/10.1016/j.bios.2014.02.009.

(4) Guo, J.; Yu, Y.; Cai, L.; Wang, Y.; Shi, K.; Shang, L.; Pan, J.; Zhao, Y. Microfluidics for Flexible Electronics. *Mater. Today* **2021**, *44*, 105–135. https://doi.org/10.1016/j.mattod.2020.08.017.

(5) Olanrewaju, A.; Beaugrand, M.; Yafia, M.; Juncker, D. Capillary Microfluidics in Microchannels: From Microfluidic Networks to Capillaric Circuits. *Lab. Chip* **2018**, *18* (16), 2323–2347. https://doi.org/10.1039/C8LC00458G.

(6) Yafia, M.; Ymbern, O.; Olanrewaju, A.; Parandakh, A.; Kashani, A. S.; Renault, J.; Jin, Z.; Kim, G.; Ng, A.; Juncker, D. Microfluidic Chain Reaction of Structurally Programmed Capillary Flow Events. **2022**. https://doi.org/10/gqmxh6.

(7) Macdonald, N. P.; Cabot, J. M.; Smejkal, P.; Guijt, R. M.; Paull, B.; Breadmore, M. C. Comparing Microfluidic Performance of Three-Dimensional (3D) Printing Platforms. *Anal. Chem.* **2017**, *89* (7), 3858–3866. https://doi.org/10.1021/acs.analchem.7b00136.

(8) Au, A. K.; Lee, W.; Folch, A. Mail-Order Microfluidics: Evaluation of Stereolithography for the Production of Microfluidic Devices. *Lab. Chip* **2014**, *14* (7), 1294–1301. https://doi.org/10.1039/C3LC51360B.

(9) Rogers, C. I.; Qaderi, K.; Woolley, A. T.; Nordin, G. P. 3D Printed Microfluidic Devices with Integrated Valves. *Biomicrofluidics* **2015**, *9* (1), 016501. https://doi.org/10.1063/1.4905840.

(10) Shallan, A. I.; Smejkal, P.; Corban, M.; Guijt, R. M.; Breadmore, M. C. Cost-Effective Three-Dimensional Printing of Visibly Transparent Microchips within Minutes. *Anal. Chem.* **2014**, *86* (6), 3124–3130. https://doi.org/10.1021/ac4041857.

(11) Gong, H.; P. Bickham, B.; T. Woolley, A.; P. Nordin, G. Custom 3D Printer and Resin for 18 Mm × 20 Mm Microfluidic Flow Channels. *Lab. Chip* **2017**, *17* (17), 2899–2909. https://doi.org/10.1039/C7LC00644F.

(12) *CADworks3D | THE NEXT EVOLUTION IN MICROFLUIDICS*. CADworks3D. https://cadworks3d.com/ (accessed 2023-09-13).

(13) Junk, S.; Bär, F. Design Guidelines for Additive Manufacturing Using Masked Stereolithography mSLA. *Procedia CIRP* **2023**, *119*, 1122–1127. https://doi.org/10.1016/j.procir.2023.01.022.

(14) Bertsch, A.; Jézéquel, J. Y.; André, J. C. Study of the Spatial Resolution of a New 3D Microfabrication Process: The Microstereophotolithography Using a Dynamic Mask-Generator Technique. *J. Photochem. Photobiol. Chem.* **1997**, *107* (1), 275–281. https://doi.org/10.1016/S1010-6030(96)04585-6.

(15) Ohshima, H. 8.1: Invited Paper: Value of LTPS: Present and Future. *SID Symp. Dig. Tech. Pap.* **2014**, *45* (1), 75–78. https://doi.org/10.1002/j.2168-0159.2014.tb00021.x.

(16) Ahmed, I.; Sullivan, K.; Priye, A. Multi-Resin Masked Stereolithography (MSLA) 3D Printing for Rapid and Inexpensive Prototyping of Microfluidic Chips with Integrated Functional Components. *Biosensors* **2022**, *12* (8), 652. https://doi.org/10.3390/bios12080652.

(17) Vedhanayagam, A.; Golfetto, M.; Ram, J. L.; Basu, A. S. Rapid Micromolding of Sub-100 Mm Microfluidic Channels Using an 8K Stereolithographic Resin 3D Printer. *Micromachines* **2023**, *14* (8), 1519. https://doi.org/10.3390/mi14081519.
(18) Poskus, M. D.; Wang, T.; Deng, Y.; Borcherding, S.; Atkinson, J.; Zervantonakis, I. K. Digital Light Processing 3D Printing for Biological Applications of Polydimethylsiloxane-Based Microfluidics. bioRxiv September 30, 2022, p 2022.09.28.509779. https://doi.org/10.1101/2022.09.28.509779.
(19) Karamzadeh, V.; Sohrabi-Kashani, A.; Shen, M.; Juncker, D. Digital Manufacturing of Functional Ready-to-Use Microfluidic Systems. *bioRxiv* **2023**, 2023.05.08.539659. https://doi.org/10.1101/2023.05.08.539659.
(20) Katsuyama, Y.; Kudo, A.; Kobayashi, H.; Han, J.; Chen, M.; Honma, I.; Kaner, R. B. A 3D-Printed, Freestanding Carbon Lattice for Sodium Ion Batteries. *Small Weinh. Bergstr. Ger.* **2022**, *18* (29), e2202277. https://doi.org/10.1002/smll.202202277.
(21) Gallastegui, A.; Dominguez-Alfaro, A.; Lezama, L.; Alegret, N.; Prato, M.; Gómez, M. L.; Mecerreyes, D. Fast Visible-Light Photopolymerization in the Presence of Multiwalled Carbon Nanotubes: Toward 3D Printing Conducting Nanocomposites. *ACS Macro Lett.* **2022**, *11* (3), 303–309. https://doi.org/10.1021/acsmacrolett.1c00758.
(22) Lo Giudice, A.; Ronsivalle, V.; Rustico, L.; Aboulazm, K.; Isola, G.; Palazzo, G. Evaluation of the Accuracy of Orthodontic Models Prototyped with Entry-Level LCD-Based 3D Printers: A Study Using Surface-Based Superimposition and Deviation Analysis. *Clin. Oral Investig.* **2022**, *26* (1), 303–312. https://doi.org/10.1007/s00784-021-03999-1.
(23) Caprioli, M.; Roppolo, I.; Chiappone, A.; Larush, L.; Pirri, C. F.; Magdassi, S. 3D-Printed Self-Healing Hydrogels via Digital Light Processing. *Nat. Commun.* **2021**, *12* (1), 2462. https://doi.org/10.1038/s41467-021-22802-z.
(24) *ANYCUBIC Photon mono X 6K-English-V0.0.1.pdf*. Google Docs. https://drive.google.com/file/u/2/d/16UlhDdbRr4DlutKSVdKVe62fp9WzVxKX/view?usp=sharing&usp=embed_facebook (accessed 2023-09-13).
(25) *Phrozen Sonic Mini 8K Resin 3D Printer*. Phrozen Technology. https://phrozen3d.com/products/phrozen-sonic-mini-8k-resin-3d-printer (accessed 2023-09-13).